

## Chapter 2

# Durability under Mechanical Load – Micro-crack Formation (Ductility)

Gideon P.A.G. van Zijl

**Abstract** A significant modification of the mechanical behaviour of cement composites is brought about by fibre reinforcement. The most important feature is crack bridging by fibres. This leads to pseudo strain-hardening in SHCC. The important feature to be considered for durability design of SHCC, which is the focus in this report, is the crack-control exhibited by this class of materials in the strain-hardening phase. The crack control in SHCC subjected to mechanical actions leading to direct tension, but also shear and compression is described here. Short term monotonic actions, long-term actions as well as cyclic actions are discussed. Another mechanical degradation process, namely that of abrasion is described. Finally, self-healing of SHCC is discussed as a promising durability feature of degradation reversal.

**Key words:** strain-hardening cement-based composites (SHCC), durability, micro-crack, mechanical load, creep, fatigue, abrasion, self-healing

## 2.1 Introductory Remarks

An important phenomenon of structural durability is the limitation of crack width, whereby ingress of potentially damaging salts, through media of moisture and gases may occur. In steel reinforced composites, the well-known danger of steel corrosion is a major source of rehabilitation/restoration cost in reinforced concrete (RC) buildings. By limiting crack widths, this source of damage and associated repair cost can be limited, or delayed, whereby repair/maintenance intervals may be increased and life cycle cost of such structures reduced. Carino and Clifton (1995) summarise crack widths in RC, as prescribed by various design codes for limitation of ingress.

In strain-hardening cement-based composites (SHCC) the tensile ductility is caused by the formation of multiple cracks. This is a process of crack control. The

---

Gideon P.A.G. van Zijl

Civil Engineering Department, Stellenbosch University, South Africa

*G.P.A.G. van Zijl and F.H. Wittmann (eds.), Durability of Strain-Hardening Fibre-Reinforced Cement-Based Composites (SHCC), 9–39.*

© RILEM 2011

crack widths are limited by the fibre pull-out resistance, whereby other matrix cracks arise, rather than widening of existing cracks. This is in contrast to normal concrete or normal fibre reinforced concrete that exhibits tension-softening, wherein fracture localization occurs once a crack is formed, so that the crack width is unlimited as load capacity decreases. The micromechanical requirements for optimizing this process have been elaborated elsewhere (Li, 1998; Kanda and Li, 1998). While it is not appropriate to repeat the micromechanical base of this class of materials here in detail, it is essential to consider the main mechanisms and parameters which govern the behaviour of these materials under mechanical and environmental actions. This allows objective characterization of the durability of SHCC. In this light the influence of amongst others, fibre type and volume, fibre aspect ratio, matrix composition for its role in determining matrix toughness and strength, as well as fibre-matrix interaction is surveyed and reported. Keeping in mind these parameters, this chapter describes the current state of knowledge of tensile deformation, the possibility of expressing it as tensile strain although it manifests as multiple cracks of finite width, the influence such cracks have on permeability to moisture and gas penetration and finally, the potential of crack healing.

It must be noted that SHCC is a young class of materials in a dynamic development phase internationally. Whilst the basic principles of achieving the required, distinguishing mechanical behaviour of SHCC have been defined, many possibilities of ingredient choice and proportioning exist, rendering the complete characterization of the durability of SHCC virtually impossible at this stage of development. Nevertheless, in the light of the stated parametrisation, generality is introduced as far as possible in the discussions of the current state-of-the-art of the durability of SHCC.

## **2.2 Ductility as Compared with the Sum of Possibly Imposed Strains**

It has been pointed out above that ductility of SHCC is not due to plastic deformation (as in ductile metal attributed to dislocation movement) but due to the formation of multiple micro-cracks. This automatically means that the material is progressively damaged in the strain hardening range. This damage can be observed as a noticeable decrease of the elastic modulus for instance. As long as the width of the micro-cracks remains below a critical value (in many cases below 40  $\mu\text{m}$ ), however, the permeability of the cement-based material is not substantially increased. In addition these fine micro-cracks will be closed under favourable environmental conditions again by self-healing. Therefore, with respect to durability, we have to require that the sum of all possibly imposed strains (strain-demand) does not exceed the tensile strain at ultimate load (strain-capacity) so that fracture localization is prevented. In addition, the micro-cracks formed during strain-hardening must not be wider than a critical crack width. Then and then only durability is not affected by imposed

strains. The critical crack width has to be determined experimentally for a given type of environmental exposure.

In practice we have to distinguish mechanical strains and strains imposed by environmental actions. The maximum mechanical strain can be estimated from the design load and accidental additional loads. Environmental actions will usually impose hygral shrinkage and swelling strain and thermal strain. These environmentally imposed strains will often be cyclic. In the long run chemically induced strains will have to be taken into consideration in addition. Typical chemical strains are carbonation shrinkage, and swelling due to alkali silica reaction (ASR) and sulphate attack.

Hygral shrinkage strain of SHCC in a moderate climate is in the range of 0.08 to 0.12%. A temperature difference of 50°C imposes a thermal strain of about 0.05%. From these simple considerations it follows that SHCC must allow an imposed strain of at least 0.2% without formation of micro-cracks wider than the critical value. Then the sum of possibly imposed strains will not have a negative influence on durability. In many cases a more precise estimation of the possibly imposed strains will be necessary of course.

### **2.3 Average and Maximal Opening of Micro-cracks during Strain-hardening**

The multiple crack formation, accompanied by tensile pseudo strain-hardening is illustrated in Figure 1.1 in terms of a uniaxial tension test force-displacement result, translated to stress and strain. The notions of stresses and strains are reserved for continua, but are commonly used for the macroscopical description of cement-based material, despite their heterogeneous nature, containing various phases like stone, hardened cement paste and, in the case of SHCC, fibres. Nevertheless, the SHCC with finely spaced, spread-out, fine cracks beyond the elastic range can be treated as a continuum when the stresses and strains in the constitutive description of SHCC denote averages of forces and deformation over a representative volume containing many microcracks. This is particularly justifiable when the microcrack spacings are on the mm scale, and the constitutive laws are used to describe material behaviour in structures on the cm or m scale. The artificial notion of “smeared cracking”, which is conveniently used for describing localized cracking in concrete, is in fact an actual, physical phenomenon in SHCC, justifying the expression of strain in these materials.

In Figure 1.1 the typical crack pattern development with increased tensile deformation of a SHCC specimen is shown. After the first crack arises, which indicates the end of the linear stress-strain relation, more cracks arise successively at higher deformation levels. The eventual reduced resistance is introduced by exceedance of the crack bridging capacity at a particular crack, at which location the deformation subsequently localizes.

**Table 2.1** Crack width measurements in SHCC, specimen composition, size and test setup.

| Li et al. (2001) <sup>1</sup> |  |           |           |           |           |           | Weimann and Li (2003) <sup>2</sup>   | Wang and Li (2006) <sup>2</sup>      |
|-------------------------------|--|-----------|-----------|-----------|-----------|-----------|--------------------------------------|--------------------------------------|
| Ref. nr.                      | 1  | 2         | 3         | 4         | 5         | 6         | 7                                    | 8                                    |
| Cement                        | 1.0  | 1.0       | 1.0       | 1.0       | 1.0       | 1.0       | 1.0                                  | 1.0                                  |
| Water                         | 0.45   | 0.45      | 0.45      | 0.45      | 0.45      | 0.45      | 0.51                                 | 0.51                                 |
| Sand                          | 1.0  | 1.0       | 1.0       | 1.2       | 1.2       | 1.2       | 0.8                                  | 0.8                                  |
| Sand grading                  | F110   |           |           | F110      |           |           |                                      | F110                                 |
| Fly Ash                       | –  | –         | –         | –         | –         | –         |                                      | 1.2                                  |
| $V_f$                         | 2.0%   | 2.0%      | 2.0%      | 2.0%      | 2.0%      | 2.5%      | 2.0%                                 | 2.0%                                 |
| Fibre type                    | PVA  |           |           |           |           |           |                                      |                                      |
| $L_f$ (mm)                    | 12   |           |           |           |           |           |                                      | 12                                   |
| $d_f$ (μm)                    | 39   |           |           |           |           |           |                                      | 39                                   |
| $E_f$ (GPa)                   | 42.5   |           |           |           |           |           |                                      | 25.8                                 |
| Oiling agent %                | 0.3  | 0.5       | 0.8       | 0.5       | 0.8       | 0.8       |                                      | 1.2                                  |
| $\tau_0$ (MPa)                | 3.5  | 2.5       | 2.0       |           |           |           |                                      |                                      |
| $G_f$ (J/m <sup>2</sup> )     | 3.0  | 2.5       | 2.0       |           |           |           |                                      |                                      |
| $J_h$ (J/m <sup>2</sup> )     | 9.6  | 10.7      | 16.5      |           |           |           |                                      |                                      |
| $\sigma_m$ (MPa)              | 4.60±0.23                                    | 4.02±0.40 | 4.58±0.38 | 3.92±0.15 | 4.28±0.17 | 5.00±0.52 |                                      |                                      |
| $\sigma_k$ (MPa)              | 3.97±0.28                                    | 2.66±0.11 | 3.11±0.14 | 3.45±0.14 | 2.63±0.32 | 3.39±0.09 |                                      |                                      |
| $\varepsilon_m$ (%)           | 1.59±0.35                                    | 3.62±0.56 | 3.68±1.16 | 1.64±0.60 | 2.48±1.04 | 4.59±0.36 |                                      |                                      |
| $w_c$ (μm)                    | 44±7   | 52±10     | 71±9      | 45±19     | 50±9      | 58±10     | Figure 2.1a                          | Figure 2.1b                          |
| Crack spacing (mm)            | 7.5 ± 2.8                                    | 3.5 ± 2.0 | 2.5 ± 0.3 | 6.4 ± 1.0 | 3.9 ± 2.4 | 1.8 ± 0.3 |                                      |                                      |
| Specimen size (mm):           |  |           |           |           |           |           |                                      |                                      |
| Length                        | 304  |           |           |           |           |           | 304                                  | 304                                  |
| Width                         | 76.2   |           |           |           |           |           | 76.2                                 | 76.2                                 |
| Thickness                     | 12.7   |           |           |           |           |           | 12.7                                 | 12.7                                 |
| Gauge                         | 180  |           |           |           |           |           | 180                                  | 180                                  |
| length                        |  |           |           |           |           |           |                                      |                                      |
| Test age (days)               | 30   |           |           |           |           |           |                                      | 28                                   |
| Curing                        | 24h in mould, 28 d in water, 1 day air dry   |           |           |           |           |           |                                      |                                      |
| Test speed                    | 0.15 mm / minute                             |           |           |           |           |           | 0.3 mm/minute                        | 0.3 mm/minute                        |
| Crack measurement             | 50 x magnifier, after unloading <sup>1</sup> |           |           |           |           |           | Single crack continuous <sup>2</sup> | Single crack continuous <sup>2</sup> |

<sup>1</sup>The reported crack widths were measured after unloading, i.e. in the residual tensile deformation state.

<sup>2</sup>Individual cracks were monitored by video microscope during loading, at various strain levels.

Crack widths have been monitored in several experimental studies. The earliest report of crack width measurements is by Li et al. (2001), as part of a SHCC sensitivity study to the parameters fibre bond (varied by surface oiling), matrix toughness (varied by aggregate content variation) and, to a limited degree, fibre volume ( $V_f = 2.0$  or  $2.5\%$ ). The study used Polyvinyl Alcohol (PVA) fibres. Other studies that included crack width measurement were reported by Weimann and Li (2003) and Wang and Li (2006). In all of these studies PVA fibre was used. Nevertheless, the other ingredient and proportioning differences, which are summarized in Table 2.1, allow some conclusions on the crack width in SHCC as influenced by the main governing parameters. This will be discussed in the following sections.

### 2.3.1 Crack Width Evolution with Tensile Strain

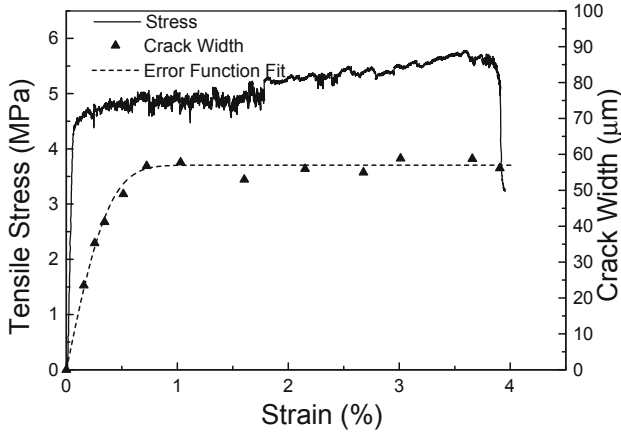
Also shown in Figure 1.1 is the crack width evolution with tensile strain. It should be noted that the crack width in that figure is that of a single crack, which was monitored throughout a uniaxial tensile test. This was done on a small rectangular tensile specimen, of dimension given in Table 2.1, as tested by Weimann and Li (2003). Similar observations were done by Li et al. (2001) and Wang and Li (2006), as shown in Figure 2.1. Note that due to fibre dispersion non-uniformity, it may be expected that crack width may vary from one crack plan to another, so that crack width on a given specimen is not a single number, but shows a statistical distribution.

It appears that, for the particular types of SHCC tested thus far, all containing PVA fibres in the range  $2.0\% \leq V_f \leq 2.5\%$  and similar matrices as indicated in Table 2.1, the crack width is arrested at a strain level of less than 1% at an average value in the range of 50–60  $\mu\text{m}$ . Subsequently, more cracks arise in the specimen upon increased tensile straining, while widening of the existing cracks is negligible. It is postulated that a crack width increase must take place to develop the higher crack bridging resistance demanded at increased tensile strain, to realise the pseudo strain-hardening behaviour. Either fibre slip or fibre stretching or both can lead to such increased resistance. From the shown crack measurements this effect appears to be insignificant.

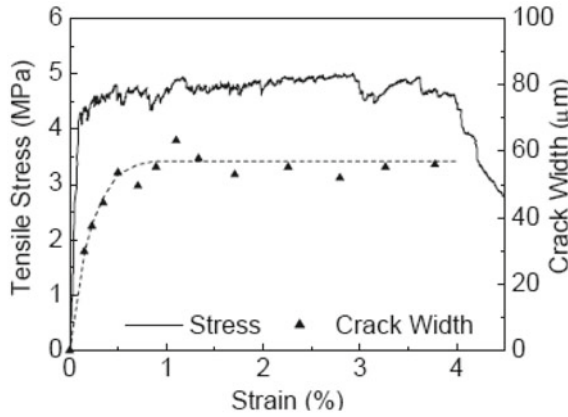
### 2.3.2 Fibre Volume

The only direct comparison is possible from the research results of Li et al. (2001), who tested similar PVA-SHCC specimens with  $V_f = 2\%$  and  $V_f = 2.5\%$ , as listed in Table 2.1 under reference numbers 5 and 6. Whereas the fibre volume increase led to increases in both the ductility, in terms of the ultimate tensile strain, and the ultimate tensile strength, the crack width changed insignificantly. Note that these crack widths were measured on specimens in the unloaded state, after a monotonic tensile test up to and beyond the ultimate strength. This means that the crack widths on the lower fibre volume specimens occurred at a significantly lower residual tensile strain level, in the region of 2%, than the higher fibre volume specimens (in the region of 4%).

This result agrees with the concept of crack width arrest in SHCC, after which more cracks arise, rather than widening of individual cracks. Arguably, at a higher fibre volume the crack opening displacement to achieve the required crack bridging strength for subsequent cracks to form will be lower, due to a larger number of fibres bridging the crack in a matrix otherwise identical. If fibre interaction is ignored, the crack width reduction should be proportional to ratio of the fibre volumes, i.e. the crack width for  $V_f = 2.5\%$  should reduce to 80% of that for  $V_f = 2.0\%$  at the same stress level. This remains to be confirmed in future test programs.



(a) Li et al. (2001)



(b) Wang and Li (2006)

**Fig. 2.1** Width evolution of an individual microcrack under uniaxial tension.

### 2.3.3 Fibre Bond Strength

Evaluation of this influence is possible by comparison of the results for specimens with reference numbers 1–3 in Table 2.1. For these specimens, the frictional fibre bond ( $\tau_0$ ) was reduced from  $\tau_0 = 3.5$  MPa (0.3% coating) to  $\tau_0 = 2.0$  MPa (0.8% coating), while the chemical bond ( $G_d$ ) was reduced from 5.0 to 2.5 J/m<sup>2</sup> for the coinciding increased oil coating level. These results were established by single fibre pull-out tests (Li et al., 2001). This realises in an increased complementary energy of the fibre bridging stress-crack opening response ( $J'_b$ ), Figure 2.2.

From the resulting crack width and spacing measurements in Table 2.1 for these specimen types it is clear that the reduced fibre bond leads to a reduced crack spa-

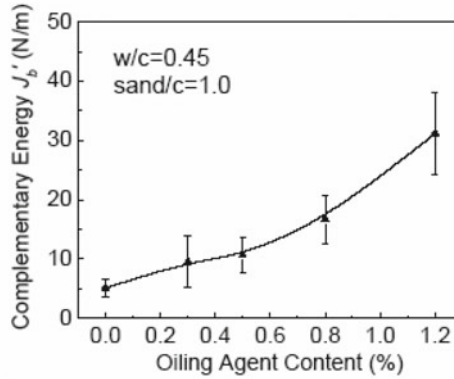


**Fig. 2.2** Fibre bridging stress-crack opening complementary energy ( $J'_b$ ) increase with PVA fibre oil coating level increase (Wang and Li, 2006).

cing (from 7.5 to 2.5 mm), although the average crack width is increased from 44 to 71  $\mu\text{m}$ . It must be noted once again that the crack widths were measured after removal of the load, which means that the residual tensile strain level was significantly lower ( $\varepsilon_{tu} = 1.6\%$ ) for specimens with the high fibre bond than for those with weaker fibre bond ( $\varepsilon_{tu} = 3.7\%$ ).

It is postulated that the fibre bond strength governs the ductility for this class of SHCC, rather than the crack width in the strain hardening phase. Thus, for objective characterisation of the influence of the fibre bond strength on the crack width evolution in SHCC, crack width measurements should be done at the same strain levels.

### 2.3.4 Influence of Matrix Composition

From the current level of micromechanical understanding and modelling, the governing parameters in the mechanical response of SHCC are the fibre factors such as fibre volume  $V_f$ , fibre length  $L_f$ , fibre diameter  $d_f$ , fibre strength and stiffness, the matrix factors such as strength, matrix toughness and maximum aggregate size (initial flaw size), and the fibre-matrix interfacial properties reflected by the frictional and chemical bond. In each of these groups of parameters, several variations are possible. In this section the influence of the matrix composition on the crack width is discussed.

Note that reference is often made to the fibre factor (FF), which combines fibre volume, length and diameter as follows

$$\text{FF} = V_f \frac{L_f}{d_f} \quad (2.1)$$

### 2.3.4.1 Aggregate Content

Whereas the role of aggregate in the tensile mechanical behaviour of certain types of SHCC has been studied intensely (Li et al., 1995, 2001; van Zijl, 2005), not sufficient crack measurements are available to draw conclusions on its influence on crack width evolution. It has been clearly demonstrated that the matrix strength, expressed by the first cracking strength ( $\sigma_{fc}$ ), and toughness, expressed by the crack tip toughness ( $J_{tip}$ ), are increased with increased sand content. Thereby tensile ductility is reduced for a given fibre factor. It has been demonstrated theoretically that the ratio between the complementary energy ( $J'_b$ ) of the fibre bridging stress-crack opening, to the matrix crack tip toughness must be larger than one for strain hardening, i.e.  $J'_b/J_{tip} > 1$ . However, the requirement for this ratio has been measured to be  $J'_b/J_{tip} \geq 3$  (Kanda and Li, 1999) for multiple cracking saturation, reflecting material variability not accounted for in theoretical models.

From the available data in Table 2.1, in particular specimens numbers 2 and 4, the reduced tensile ductility is confirmed with even a slight increase in aggregate to cement proportion from 1.0 to 1.2. Nevertheless, the average crack width is insignificantly changed, keeping in mind the different residual strain levels at which they were measured. However, the crack spacing is nearly doubled with this increase in aggregate content.

### 2.3.4.2 Cement Replacement by Fly Ash and Slagment

The role of fly ash (FA) in the mechanical behaviour of certain classes of SHCC has been studied by several research groups, for example Peled and Shah (2003), Song and van Zijl (2004), Wang and Li (2006). Cement replacement with FA has been shown to reduce the matrix strength, seen in Figure 2.3 for specimens with FA/C = 1.4. It has been postulated that the fibre-matrix interfacial zone is modified, leading to improved fibre slip from the matrix instead of fibre breakage. Measurements show reduced chemical bond but higher frictional bond with increase of fly ash. Thus both matrix and interface properties are modified, illustrated by the increased ratio  $J'_b/J_{tip}$  in Figure 2.4 (Wang and Li, 2006).

In contrast, cement replacement with large quantities (up to 50% by mass) of ground granulate Corex slagment (slag), led to a strong matrix (Figure 2.3). Of importance here is the crack patterns associated with these classes of SHCC. Although the crack widths were not measured, it is clear that the crack width and spacing are significantly larger for the slag-SHCC than for FA-SHCC. Note that the mix design for these specimens was otherwise similar in terms of fibre type (PVA,  $L_f = 12$  mm,  $d_f = 40$   $\mu$ m) and volume (2.5%), aggregate content (aggregate/binder = 0.5) as well as water content (water/binder = 0.4).

Consider the crack width measurements for the specimens with reference number 8, Table 2.1 and Figure 2.1b. These specimens, containing large quantities of FA, show comparable crack widths with those of specimens without FA. As a general indication, the large stress fluctuations seen in Figure 2.3 (top) are indicative of lar-



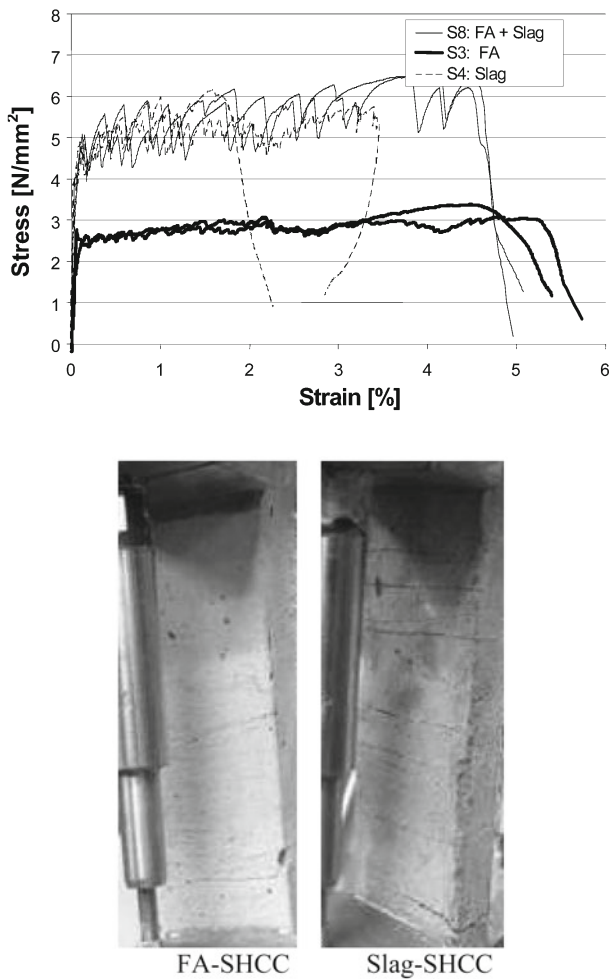


**Fig. 2.3** Tensile stress-strain responses of FA-SHCC and slag-SHCC (Song and van Zijl, 2004).

ger crack widths. This may even occur in matrices without slag, but for composites with fibre volume approaching the critical level for pseudo strain-hardening.

### 2.3.5 Age at Loading, Curing

It must be noted that the crack width determination was on relatively young specimens, loaded 28 days after casting. There is evidence that SHCC becomes more brittle with aging, as found in the results of direct tensile testing at various ages of PVA-SHCC by Wang and Li (2005), as well as Lepech and Li (2005). Due to the

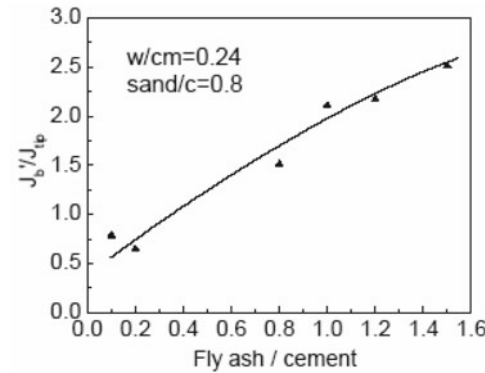


**Fig. 2.4** FA content driven improvement of complementary energy: toughness ratio, critical for multiple, fine cracking (Wang and Li, 2005). The mix contained PVA fibre at  $V_f = 2\%$ , 1.2% oil coating.

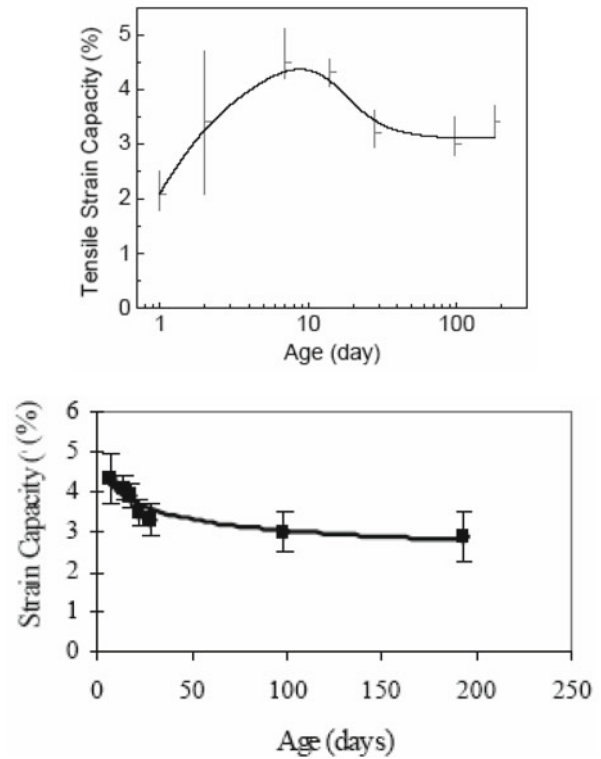


**Fig. 2.5** Reduction in tensile strain capacity with aging of SHCC by (top) Wang and Li (2005) and (bottom) Lepech and (Li 2005).

delicate balance of binder matrix, fibre, and matrix/fibre interface properties, the strain capacity of SHCC changes during maturing. A gradual decrease of this value was observed by Li and Lepech (2005) from approximately 5% at the age of 10 days to approximately 3% at the age of 180 days, which is a result of the continued hydration process. Figure 2.5 shows the reduced tensile strain capacity with increased loading age of specimen reference number 8 in Table 2.1. This figure also shows that the material reaches a steady state strain capacity value at approximately 3% after about 80 days. As an important mechanism of tensile strain capacity, multiple crack formation must lie at the basis of this aging symptom. It remains to be verified on older specimens whether crack widths are indeed arrested and to what crack width level.

### ***2.3.6 Crack Formation in Shear***

The intrinsic crack control of SHCC may be beneficial in applications where tensile or pure flexural conditions dominate, but crack control also in other, more general conditions, including shear, will extend its applicability. It will be argued in subsequent sections that if cracks are controlled to within a threshold level below which ingress rates of water, gas and chlorides are insignificant, durability of cement-based composites, and particularly SHCC and R/SHCC is improved.

Li et al. (1994) executed Ohno-type shear beam tests (Arakawa and Ohno, 1957) on SHCC containing 2% by volume high molecular weight Polyethylene fibre (SPECC). This SHCC contained no sand, but only cement paste with water:cement mass ratio of 0.27. For comparison several other beams were tested, fabricated of plain concrete (PC), reinforced concrete (RC), FRC (1% by volume steel fibres) and DRECC, containing a similar cement paste as the SPECC, but with 7% by volume Dramix steel fibre (6 mm  $\times$  0.15 mm diameter, brass coated steel fibres).

Figure 2.6 shows the setup, as well as average shear stress-strain results, including crack width evolution. The PC results have been omitted, as it fails immediately at first crack. In the RC specimen two large diagonal cracks are formed at a load level approximately equal to the failure load of the PC specimen. The crack widths at this load are in the range from 0.1 to 1 mm. At the peak load, a third large crack forms suddenly due to failure of the bond between the steel shear reinforcement and the concrete. In the FRC specimen a large diagonal crack formed just after first crack, of which the width was in the range 0.1 to 1 mm, which is beyond the threshold level of insignificant penetration rate of water gas and chlorides. In the two SHCC specimens (SPECC, DRECC), cracks with width smaller than 0.1 mm developed in the strain hardening region following first cracking. In this region a large number of small cracks were formed in SPECC. Thus evidence has been presented that the multiple, controlled cracking described under tension and flexure is retained under shear.

Van Zijl (2007) derived an appropriate geometry for an SHCC Iosipescu-type shear test (Iosipescu, 1967). By the derivation of an appropriate geometry, with spe-

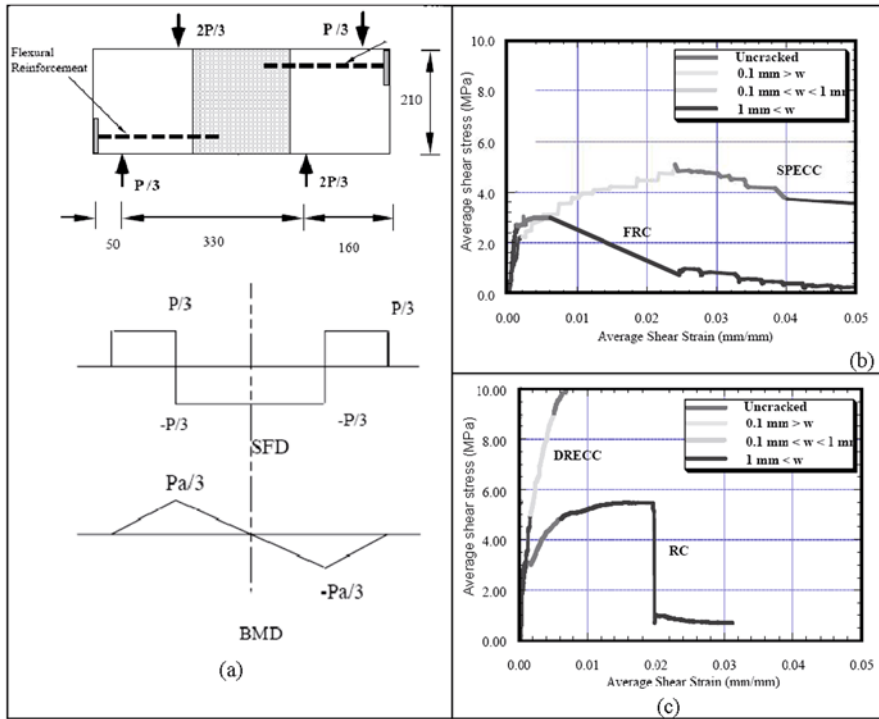


**Fig. 2.6** Ohno-type shear test setup for SHCC and other beams by Li et al. (1994). Dimensions in mm.

cial care for the notch geometry, an approximately uniform shear stress distribution is induced along the specimen height at the position of pure shear (zero bending moment). In addition, the risk of failure in bending away from the pure shear section is reduced, whereby the pure shear behaviour can be studied in the elastic, but also the post first cracking region and eventual localisation in the pure shear plane. The setup is shown in Figure 2.7.

A test series was performed on specimens containing ingredients listed in Table 2.2, containing a small amount of ground granular corex slag (GGCS) and various levels of PVA fibre volume proportions ( $L_f = 12 \text{ mm}$ ,  $d_f = 40 \mu\text{m}$ ). The results clearly showed that the multiple, fine cracking to a width below the durability threshold is retained in pure shear of SHCC, i.e. for specimens with  $V_f = 2\%$  and  $V_f = 2.5\%$ .

**Table 2.2** SHCC shear specimens mix ingredients and proportions by mass (van Zijl, 2007).

|    | Cement | Fly Ash | GGCS | Water | Sand | $V_f$ (%) |
|----|--------|---------|------|-------|------|-----------|
| S1 | 0.5    | 0.45    | 0.05 | 0.4   | 0.5  | 0         |
| S2 | 0.5    | 0.45    | 0.05 | 0.4   | 0.5  | 1         |
| S3 | 0.5    | 0.45    | 0.05 | 0.4   | 0.5  | 2         |
| S4 | 0.5    | 0.45    | 0.05 | 0.4   | 0.5  | 2.5       |

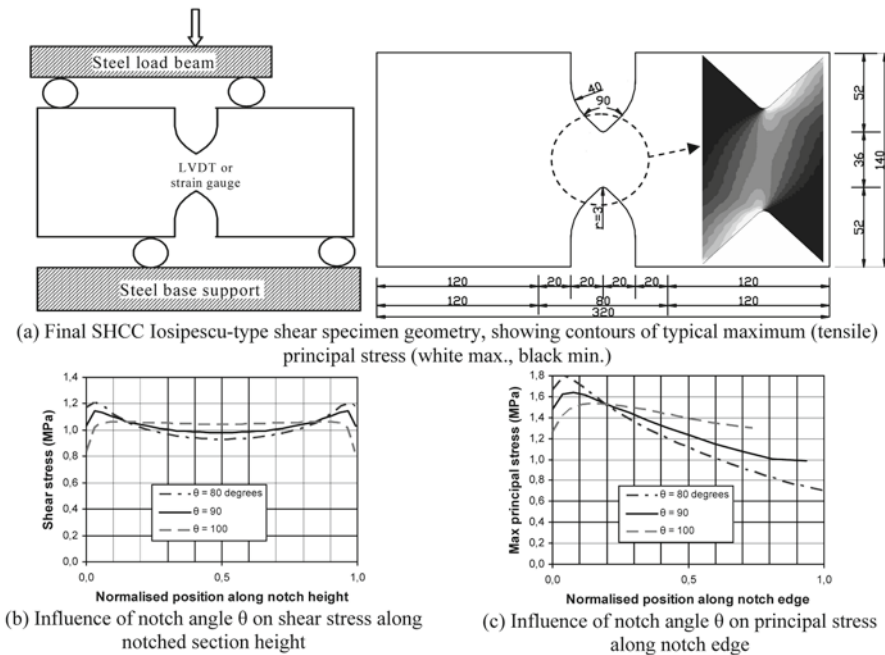


**Fig. 2.7** Iosipescu-type shear test setup for SHCC by van Zijl (2007).

**2.4 Width of Micro-cracks in Loaded and Unloaded Specimens**

The crack width measurements reported in Section 2.2 have been either on specimens in the loaded state (reference specimens numbers 7, 8 in Table 2.1) or after unloading (reference numbers 1–6 in Table 2.1). Furthermore, the measurements in the unloaded state were at different permanent deformation levels for different specimens. However, continuous monitoring of single cracks during the loading phase of reference number 6 is shown in Figure 2.1b. The crack width of the single crack monitored during loading, which stabilises at a width in the range 50–60  $\mu\text{m}$ , is comparable with the average width measured in the unloaded state (58  $\mu\text{m}$ ). However, this effect remains to be studied in a systematic way, measuring crack widths at similar deformation levels in the loaded and unloaded state.

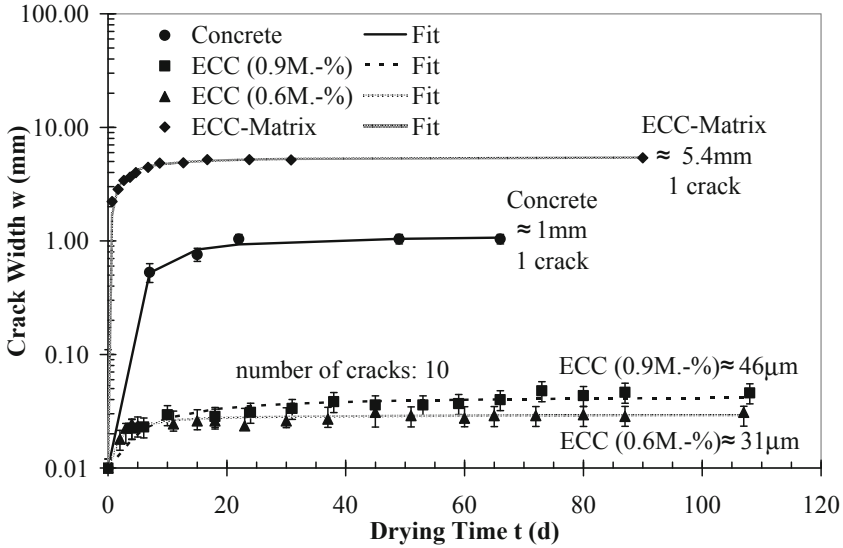
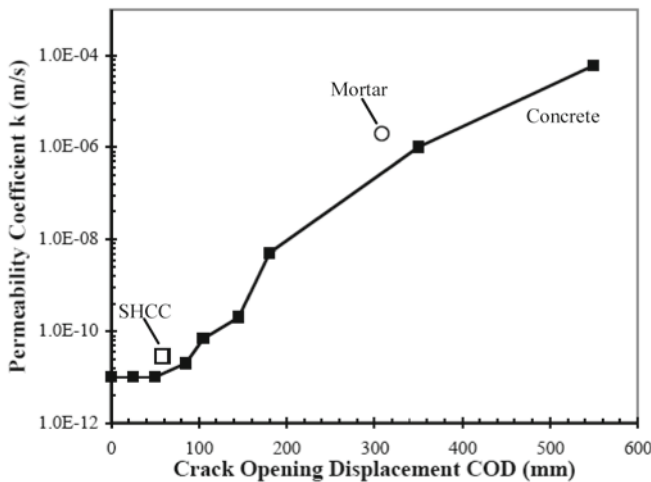


**Fig. 2.8** Crack width evolution of SHCC (mix reference number 7, Table 2.1) in drying shrinkage ring test (Weimann and Li, 2003).

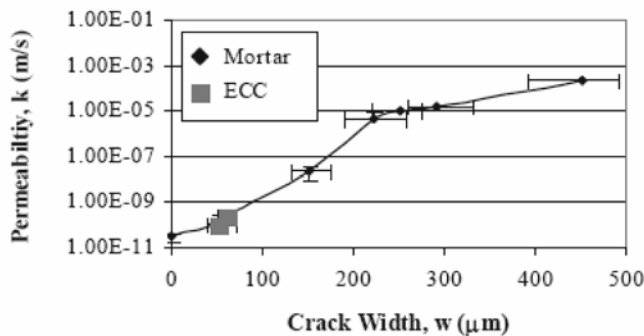
An indication of crack width under load is given by the average crack widths measured on specimens of mix reference number 7 in Table 2.1, subjected to restrained drying shrinkage in a restrained shrinkage ring test (Weimann and Li, 2003). Separate, free shrinkage tests indicated that the maximum drying shrinkage strain of this SHCC composite is in the range from 0.17 to 0.25% when drying from saturation (100% moisture content) to 0% moisture content. Under similar environmental conditions, cracks of average width  $46 \mu\text{m}$  were measured for this material in the ring shrinkage test (Figure 2.8).

## 2.5 Influence of Crack Width of Micro-cracks on Permeability and Capillary Suction

Resistance to moisture, gas and salt penetration is an important mechanism of cement-based materials durability. Either the material degradation or reinforcing steel corrosion may be consequences of such ingress. Resistance to moisture, gas and chloride ingress is a measure of the susceptibility of SHCC to such degradation processes. General consensus exists that capillary sorption and moisture diffusion are models describing the most important mechanisms of moisture ingress and migration. In the near surface zone capillary sorption dominates moisture intake (Neithalath, 2006) while moisture diffusion governs the longer term migration of water in the material through the micro-pores (Bažant and Najjar, 1971; Neithalath, 2006). By matrix densification the capillary absorption is significantly reduced in



(a) Concrete (Wang et al., 1997) and SHCC (reference number 8, Table 2.1, Li and Stang, 2004)



(b) ECC (SHCC reference number 8, Table 2.1) and steel wire mesh reinforced mortar (Lepech and Li, 2005)

**Fig. 2.9** Water permeability as function of crack width of cement-based composite materials.

UHPFRC (Kunieda et al., 2007). In SHCC diffusivity is reduced by inherent crack control (Lepech and Li, 2005; Sahmaran et al., 2007).

### 2.5.1 Water Permeability

Whereas permeability to water, gas and chlorides in the virgin state is an indication of material durability, exploitation of the superior mechanical qualities of SHCC will lead to microcracking in the service state in structural applications of these ma-

terials. The significance of crack width with regard to water permeability has been studied for concrete (Wang et al., 1997). The water permeability of concrete was shown to decrease by seven orders of magnitude as the crack width decreases from 550 to below 100  $\mu\text{m}$  (Figure 2.9). Li and Stang (2004) found that the permeability of cracked SHCC of type reference number 8 in Table 2.1, as well as a cracked steel wire mesh reinforced (2.9%) mortar are in reasonable agreement with the permeability of cracked concrete, when both have the same laboratory controlled crack width. This is shown in Figure 2.9a. Lepech and Li (2005) also performed water permeability studies for steel wire mesh reinforced mortar cracked to various crack width levels, confirming the dominance of the crack width on permeability control, as opposed to the cement-based composite type. These results are shown in Figure 2.9b. The permeability study of cracked SHCC and mortar was performed on specimens of dimension 75 mm  $\times$  180 mm  $\times$  12 mm which had been pre-cracked in a uniaxial tensile test up to a tensile strain of 1.5%.

It must be noted that the number of cracks in the specimen represented in Figure 2.9a differ. The imposed tensile deformation resulted in 10 cracks of approximately 300  $\mu\text{m}$  width in the reinforced mortar, as opposed to 50 cracks of average width 60  $\mu\text{m}$  in SHCC. In Figure 2.10 the total permeability and the permeability normalised by the number of cracks in the specimen are compared for ECC (SHCC, reference number 8, Table 2.1) and reinforced mortar at various crack width levels. Note that all these permeability tests were performed on specimens after unloading of the mechanical load, with which the cracking was imposed.

In contradiction, the flow rate was found to be lower in FRC than in plain concrete by Tsukamoto (1990), ascribing it to the increased tortuosity of the cracks in the presence of fibre. However, the difference in flow rate becomes negligible when the crack width is below 100  $\mu\text{m}$ . This threshold value is in agreement with results of permeability tests by Rapoport et al. (2001) on steel fibre reinforced concrete (SFRC). The steady state permeability of SFRC specimens, cracked by Brazilian split test to different levels of crack width, was insensitive to the fibre volume content level, for crack widths up to 100  $\mu\text{m}$ . The crack width in the SHCC in Figure 2.10 is 60 micron.

### **2.5.2 Gas Permeability**

Up to date no systematic study of permeability to gas penetration as a function of crack width has been performed for SHCC.

### **2.5.3 Chloride Permeability**

Increased crack width can be related to higher chloride penetration rate in cement composites. Chloride ingress and migration in cement composites is predominantly



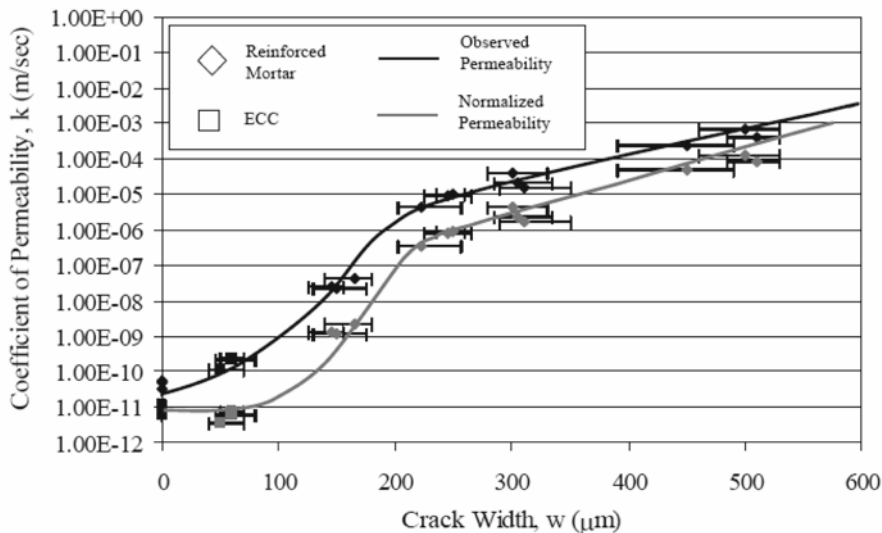


**Fig. 2.10** SHCC and steel mesh reinforced mortar water permeability normalised by the number of cracks (Lepech and Li, 2005).

as solvent in moisture, thus sharing the driving mechanisms of absorption and diffusion. Sahmaran et al. (2007) studied chloride penetration and permeability of SHCC in comparison to mortar. Based on results of immersion tests, chloride penetration depth was found to be reduced in uncracked SHCC specimens compared to uncracked mortar. Based on ponding tests of pre-cracked specimens, the effective chloride diffusion coefficient was found to be strongly dependent on crack width in mortar (Figure 2.11 a). The diffusion coefficient in SHCC was found to be comparative for equal crack widths in SHCC and mortar. However, the crack width in SHCC was found to be insensitive to the deformation level, which in this case was induced by four point bending. This explains the diversion of chloride diffusivity of mortar specimens from that of SHCC with increased deformation level (Figure 2.11 b).

The reduced penetration depth in SHCC versus reinforced mortar/concrete is confirmed by observations of Maalej et al. (2002) and Miyazato and Hiraishi (2005), in comparative SHCC and concrete beams loaded in flexure to the same deflection (see Section 3.2.1).

Sahmaran et al. (2007) performed chloride diffusion tests on preloaded beams subjected to chloride solution ponding. The effective diffusion coefficient of SHCC was found to be linearly proportional to the number of cracks (see Figure 2.12), whereas the effective diffusion coefficient of reinforced mortar is proportional to the square of the crack width. Therefore, the effect of crack width on chloride transport was more pronounced when compared to that of crack number. From the results of this study, it is concluded that SHCC is effective in slowing the diffusion of chloride ion under combined mechanical and environmental (chloride exposure) loading, by virtue of its ability to achieve self-controlled tight crack width.

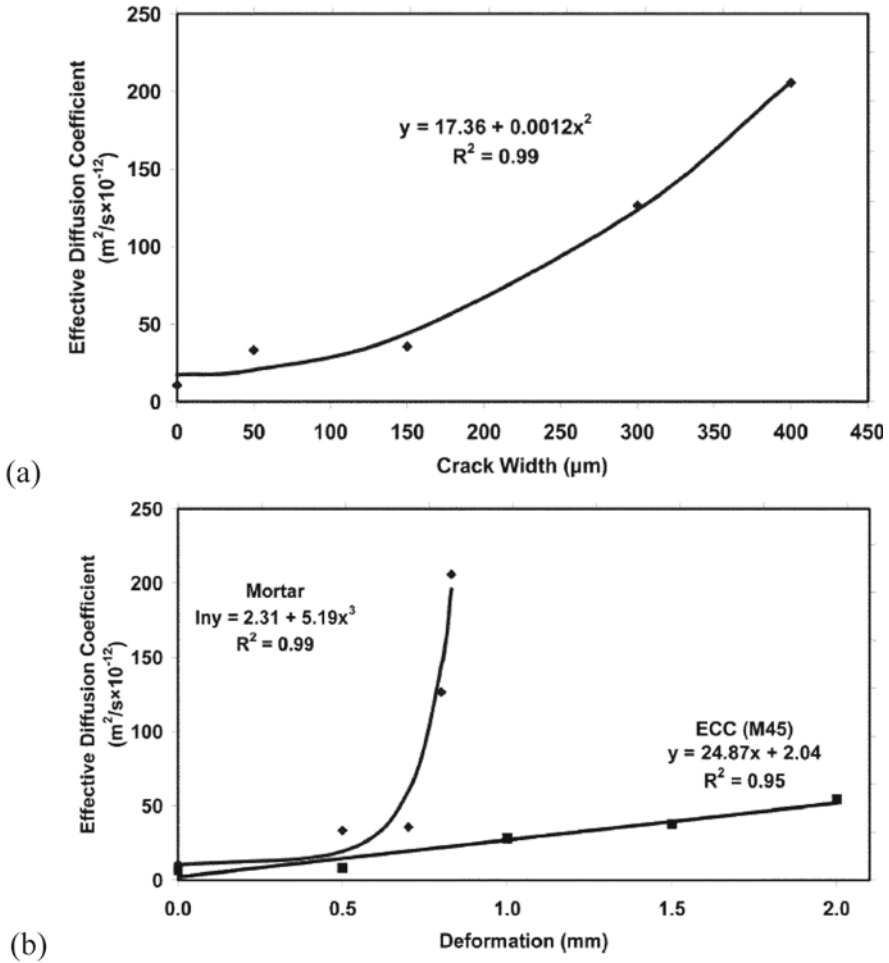


**Fig. 2.11** Diffusion coefficient versus (a) crack width for mortar deformed under bending load, (b) deflection of SHCC and steel mesh reinforced mortar (Sahmaran et al., 2007).

Oh and Shin (2006) tested SHCC to measure chloride diffusivity in cylinder specimens that were subjected to various numbers of cyclic loadings in compression. PVA fibres with a length of 12 mm and a diameter of 0.04 mm were used in the tests. The fibre content was 2% by volume. The cylinder specimens of  $\varnothing 100 \times 200$  mm were loaded in compression up to 55, 70 and 85% stress level of static strength for 1,000, 10,000 and 100,000 cycles, respectively.

After unloading, the specimens with the length of 50 mm were cut off from the central portions of the cylindrical specimens for chloride permeability tests. The chloride resistance was evaluated by the amount of charge passing through the specimens. The chloride penetration test used in this study is based on the standard of

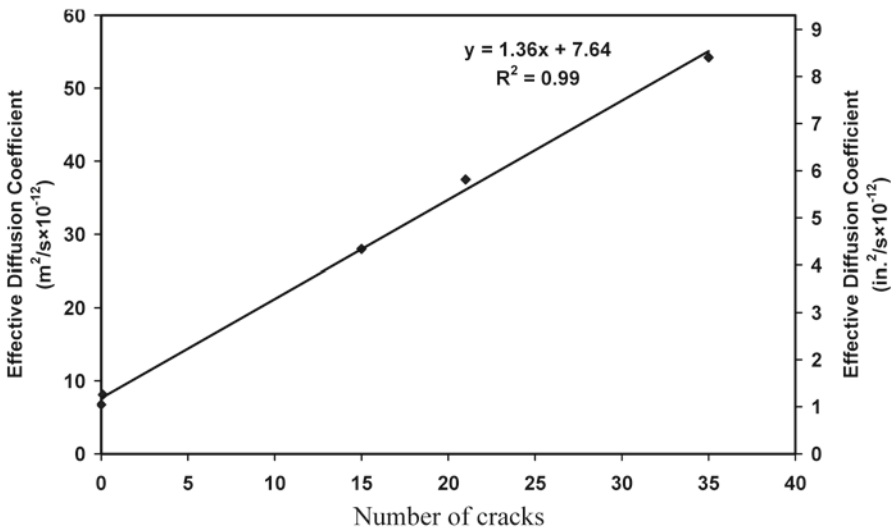


**Fig. 2.12** Effective chloride diffusion coefficient versus number of cracks for SHCC (crack width at 50 micron) (Sahmaran et al., 2007).

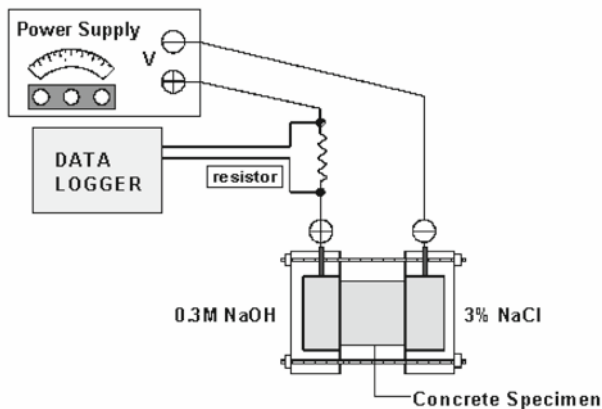


**Fig. 2.13** Test setup for measurements of chloride ion penetration (Oh and Shin, 2006).

Nord Test Build 492 – Non-Steady State Migration Test (NT BUILD 492, 1999). Figure 2.13 shows the test setup for measurement of chloride ion penetration conducted by Oh and Shin (2006).

Figure 2.14 shows the test results for the relative chloride diffusion coefficients of various specimens after applied cyclic loads. Figure 2.14 exhibits the relative ratios of residual axial strains and chloride diffusion coefficients at larger load cycles of 10,000 and 100,000 cycles to those values at 1,000 cycles under the cyclic load level 55%, respectively. It can be seen that the residual strain after 100,000 cycles at the

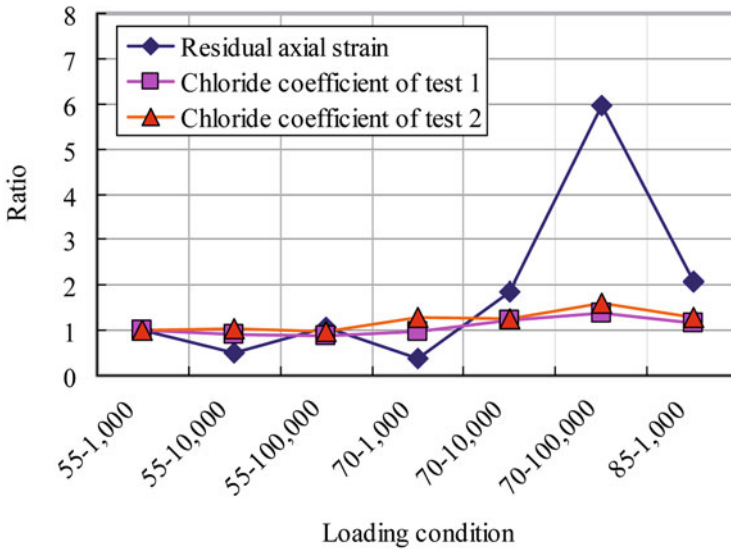


**Fig. 2.14** Relative ratios of residual strains and chloride ion penetration coefficients after cyclic loadings (Oh and Shin, 2006).

stress level of 70% is 6 times as large as that after 1,000 cycles at 55% stress level, which indicates that the specimen is significantly damaged due to a large number of repeated loading under high stress level. However, the chloride permeability coefficient is not increased as significantly as can be seen in Figure 2.14, even though the residual strain due to damage is very large. This is due to the very fine internal microcracks in the specimen that do not cause any drastic increase of permeability. This is again due to the beneficial effect of fine cracking due to high performance fibres in the specimen.

## 2.6 Sustained and Cyclic Load

It is essential that crack control is maintained in service conditions. For structures subjected to cyclic loads, or relatively high permanent/sustained loads, cracks must remain restricted to below the threshold width beyond which highly increased moisture, gas and chlorides ingress.

Figure 2.15 schematises examples of cyclic and sustained tensile loading conditions, showing also the typical response to monotonic tensile load. Jun and Mechtcherine (2007) performed such tests on SHCC under creep, as well as force and displacement-controlled cyclic loads. The number of tests under each loading condition was limited, not sufficient to give a sound statistical base. Nevertheless, their results indicate limited sensitivity to such loading conditions of the total number

of cracks that arose at the same level of total deformation. The most significant deviation was a roughly 20% lower average number of cracks under deformation controlled cyclic loading. Note that the sustained stress level and the upper tensile stress levels in the cyclic tests, are close to and above the stress at first crack.

Boshoff (2007) performed tensile creep tests on pre-cracked SHCC specimens. The specimens were subjected to a tensile deformation causing average strain of 1%. This is shown schematically in Figure 2.15b. Subsequently, tensile creep loads of 30, 50, 70 and 80% of the ultimate tensile strength were applied. This simulates a large live load which causes the SHCC member to enter the strain-hardening region, after which the live load is removed and the load drops to the respective sustained load level. In these experiments, the initiation of new cracks during the sustained load phase was observed. However, under these loading conditions, fewer cracks formed under the creep loads than under monotonic deformation-controlled tensile loading to the same level of deformation. Specifically for the high sustained load (80%), a larger crack spacing and associated wider cracks were observed. Accurate measurement of time-dependent crack width under sustained tensile load remains to be performed, and is a current research focus.

From the creep results it appears that crack initiation (see for example Figure 2.16a), width evolution as well as matrix creep contribute to creep deformation. In studying a mechanism of crack width increase under creep load, Boshoff (2007) performed single fibre pull-out tests under monotonically increasing pull-out displacement, as well as under tensile creep load. In all single fibre creep tests complete pull-out occurred, albeit delayed with up to 70 hours under a load of half the peak bond resistance. This is indication that this time-dependent fibre slip is a mechanism of tensile creep deformation, and time-dependent crack width increase.

An important further phenomenon is creep fracture, or delayed fracture of the tensile specimen subjected to sustained load. In the tests by Jun and Mechtcherine, where the tensile resistance at a strain of 1 and 2% respectively was sustained, the specimens failed after 5 and 16 hours respectively. In the tests by Boshoff (2007) creep fracture did not occur under sustained load (now already after a duration of 1.5 years), although significant deformation, beyond the monotonic tensile deformation capacity at that load, was recorded for the high sustained load cases (80% of ultimate monotonic tensile resistance). Much work still needs to be done in this area. At lower sustained load levels, it appears that creep deformation was arrested, in agreement with the so-called creep limit concept, i.e. the stress-strain response under monotonic load at infinitely slow loading rate.

## 2.7 Fatigue

Although limited results exist, fatigue behaviour of SHCC specimens in direct tension (Matsumoto et al., 2004), flexure (Suthiwarapirak et al., 2002), as well as of SHCC in composite action with concrete in overlay repair strategy (Zhang and Li, 2002), have been tested recently.

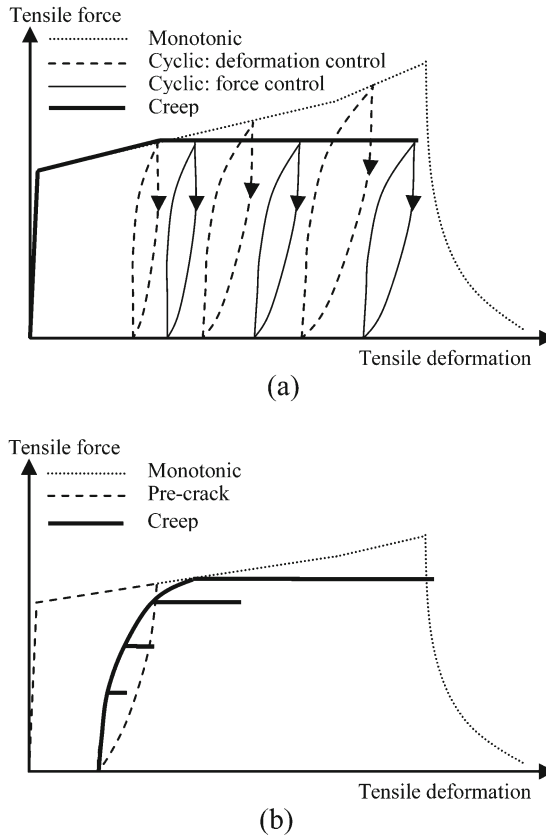


**Fig. 2.15** Tensile load cases applied by (a) Jun and Mechtcherine (2007) and (b) Boshoff (2007).

For both direct tension and flexure a reduced resistance with increased number of load cycles, characteristic of most construction materials, has been reported (see Figure 2.17). Another significant trend reported by Suthiwarapirak et al. (2002), see Figure 2.18, is the gradual increased crack width with increased number of load cycles, until eventual sudden widening when failure is imminent. Note that the total crack mouth opening displacement (TCMOD) reported by these researchers is the sum of several (up to 10) crack widths, in fact including matrix deformation between cracks, as measured by an LVDT spanning all cracks at midspan at the beam farthest tensile face. The individual CMOD was measured with the aid of a microscope at the crack that caused eventual failure. In Figure 2.18b it appears that the maximum crack width is maintained below 0.1–0.15 mm for a large range in load cycles (roughly 10,000), after which the crack widens beyond this threshold level. Note that this is for a maximum flexural stress of 70% of the flexural strength. From Figure 2.18a it appears that higher stress levels cause larger total crack width than lower stress levels.

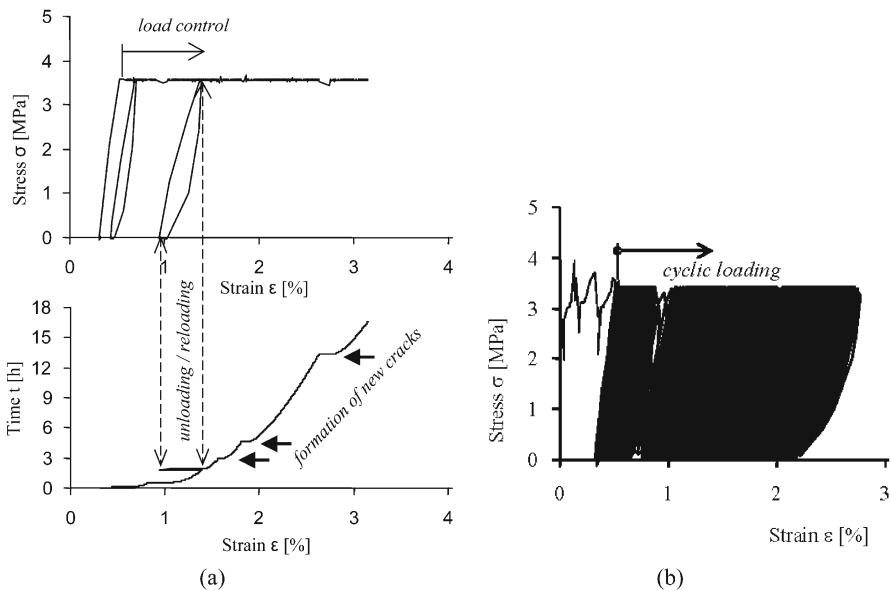


**Fig. 2.16** Representative (a) stress-strain and time-strain curves under sustained load, and (b) cyclic loading acc. to Jun and Mechtcherine (2007).

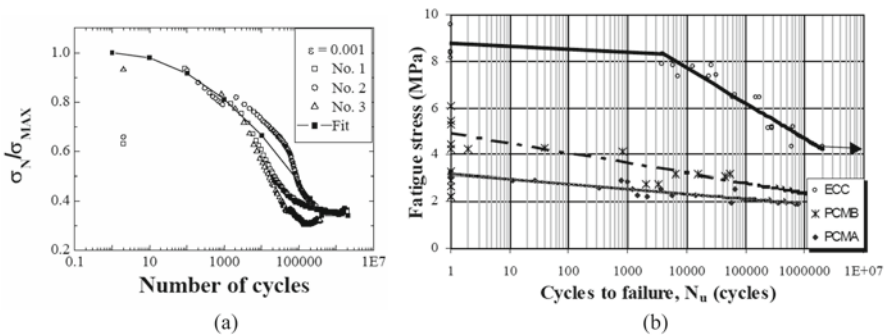


**Fig. 2.17** SHCC fatigue test results in terms of stress level – number of load cycles for (a) direct tension (under cyclic strain with strain amplitude equal to 0.1%, Matsumoto et al., 2004), and (b) flexure (four point bending, Suthiwarapirak et al., 2002). Note that the response of SHCC (ECC) is compared with two Portland cement mortars.

Zhang and Li (2002) tested an overlay repair strategy with an SHCC overlay on a concrete substrate, using simple four point bending to represent loading action on ground slabs, see Figure 2.19. A superior response to that of a concrete overlay is reported (Figure 2.19b), along with the characteristic reduced resistance with number of loading cycles.

Note that in all the above reported fatigue tests, PVA fibres of length 12 mm and diameter about 40  $\mu$ m were used, at fibre volumes of 2.0% (Zhang and Li, 2002)

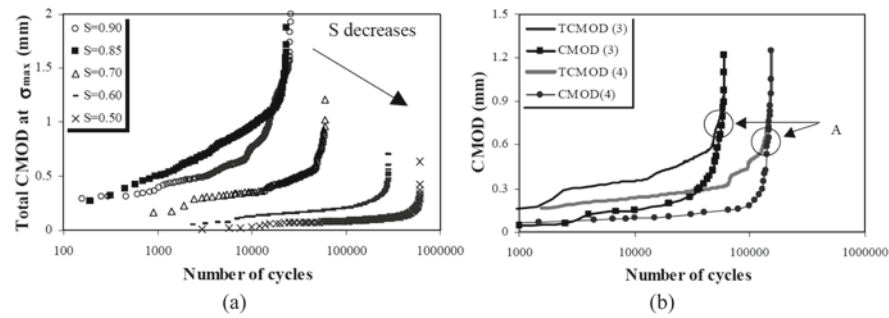


**Fig. 2.18** SHCC total crack mouth opening displacement (TCMOD) under fatigue flexural load (a) at various cyclic stress amplitudes, and (b) compared with maximum CMOD for 2 particular specimens subjected to cyclic load causing a maximum flexural stress level of 70% of the flexural strength (Suthiwarapirak et al., 2002).

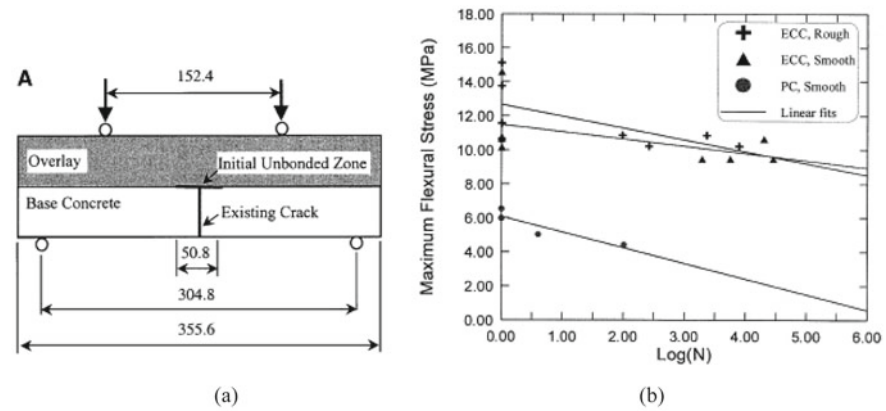


**Fig. 2.19** Flexural fatigue test of SHCC (ECC) overlay repair on concrete substrate strategy, showing characteristic reduced strength with increased number of loading cycles for an SHCC overlay, compared with a concrete overlay (Zhang and Li, 2002).

and 2.1% (Suthiwarapirak et al., 2002; Matsumoto et al., 2004) respectively. The matrices were different from those given in Table 2.1, varying in water to binder ( $w/b$ ) and sand to binder ( $s/b$ ) content ratios as follows:

- $w/b = 0.32$ ;  $s/b = 0.42$  (Figures 2.17 and 2.18; Suthiwarapirak et al., 2002; Matsumoto et al., 2004);
- $w/b = 0.434$ ;  $s/b = 1.0$  (Figure 2.19; Zhang and Li, 2002).





**Fig. 2.20** Grinding disc for abrasion testing according to the German standard (E DIN 52108 2006).

## 2.8 Abrasion

Since repair layers on horizontal concrete surfaces are a possible application of SHCC, the abrasion resistance of this material is one of the material properties to be determined.

Li and Lepech (2005) conducted both static friction testing and wear track testing according to the Michigan Test Method (MDoT, 2001). The surfaces of the tested SHCC specimens had been textured by different methods. After determining the initial static friction forces between a test tire and the wet surfaces of the test materials, the samples were subjected to 4 million tire passes. Then, the friction forces were determined again. These friction forces measured after wearing are called Aggregate Wear Index (AWI) according to the test standard (MDoT, 2001). For the differently textured SHCC samples values between 1.6 and 2.3 kN were obtained. The required minimum AWI value for Michigan amounts to 1.2 kN. It was concluded that SHCC surfaces on roadways are suitable for heavy traffic volumes.

The test method according to the German standard E DIN 52108 (2006) is significantly different from the procedure described above. It is used in European countries for measuring the abrasion resistance of cementitious materials and based upon the so-called *Böhme* grinding disc (see Figure 2.20). This testing apparatus consists of a rotating disc the specimen surface is pressed upon. Reproducible abrasion conditions are ensured by using synthetic aluminium oxide as a standardized grinding medium.

**Table 2.3** Material composition.

| Component              | Content by mass |
|------------------------|-----------------|
| CEM I 32.5 R           | 1.0             |
| Water                  | 0.9             |
| Fly ash                | 2.0             |
| Fine sand (0.1–0.5 mm) | 0.6             |
| Plasticizer            | 0.02            |
| Methyl cellulose       | 0.003           |

**Table 2.4** Experimental results.

| Age of the material | Abrasion $A$ in [ $\text{cm}^3/50 \text{ cm}^2$ ] |                   |                        |                   |
|---------------------|---|-------------------|------------------------|-------------------|
|                     | SHCC  |                   | Reference mortar       |                   |
|                     | $A_{\text{Thickness}}$                            | $A_{\text{Mass}}$ | $A_{\text{Thickness}}$ | $A_{\text{Mass}}$ |
| 14 days             | 17.2  | 17.5              | 19.6                   | 19.8              |
| 28 days             | 16.9  | 16.9              | 21.5                   | 21.9              |

The composition of the SHCC material used for abrasion testing according to the German standard is given in Table 2.3 (Wagner, 2007). PVA fibres “REC 15”, Kuraray, length 8 mm, were used with a volume content of 2.2%. This SHCC appears to have a comparably high strain capacity. It was not primarily optimized for a high abrasion resistance.

A reference mortar also tested had the same composition, but no fibre reinforcement.

The specimens had the dimensions of  $71 \times 71 \times 71 \text{ mm}^3$  according to E DIN 52108 (2006). They were cut out of cubes with an edge length of 150 mm and grinded until the prescribed dimensions were reached. Before testing, the samples were dried at  $105^\circ\text{C}$ .

The material loss due to abrasion may be quantified either by measuring the change in specimen thickness or by measuring the mass loss. Both methods have been applied. Table 2.4 contains the results obtained at the age of 14 and 28 days, respectively. Each of the abrasion values represents the material volume loss related to the surface area and is a mean value for three individual samples. It turns out that the two methods for determining the abrasion yield almost the same results.

On the basis of the experimental results, the following conclusions may be drawn:

1. The difference between the abrasion resistance after 14 and 28 days, respectively, is insignificant.
2. The abrasion of the reference mortar after 28 days was found to be about 28% higher than the one of SHCC. The PVA fibre reinforcement leads to an increase in abrasion resistance.
3. According to the European standard DIN EN 13813 (2003), the SHCC may be assigned to abrasion class A22, see Table 2.5. This is the lowest abrasion class. Accordingly, SHCC surfaces are not recommendable for heavy roadway traffic.

**Table 2.5** Abrasion classes according to DIN EN 13813 (2003).

| Class   | A22 | A15 | A12 | A9 | A6 | A3 | A1.5 |
|---|-----|-----|-----|----|----|----|------|
| Abrasion [cm <sup>3</sup> /50 cm <sup>2</sup> ] | 22  | 15  | 12  | 9  | 6  | 3  | 1.5  |

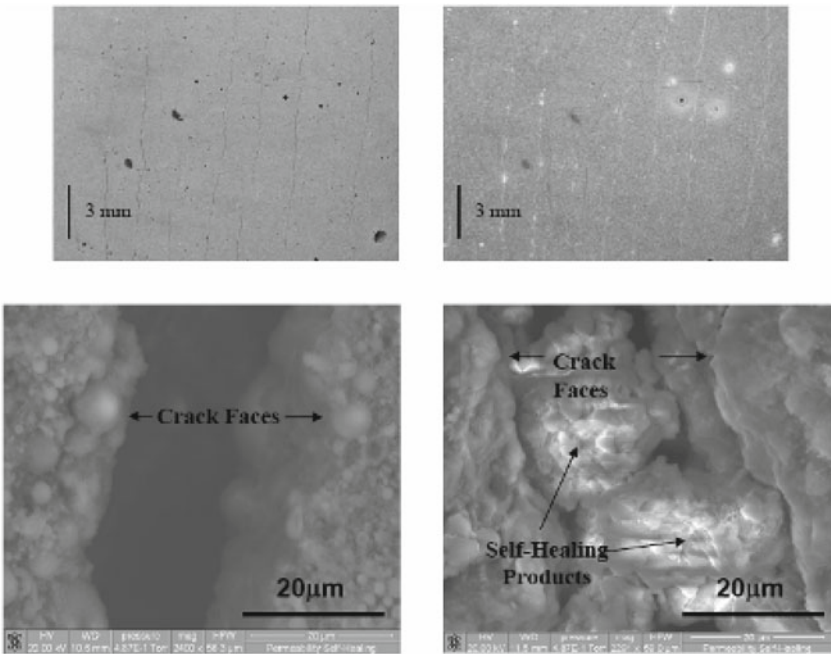


**Fig. 2.21** Images indicating self-healing product formation in SHCC (Lepech and, Li 2005).

4. The results obtained with *Böhme*'s grinding disc are contradictory to those obtained in the US according to MDoT (2001). Possibly, by using the grinding disc the abrasion resistance is underestimated. The assessment according to MDoT (2001) seems to be more realistic with respect to the actual loading of real road-way surfaces.

Generally, a high abrasion resistance of cementitious materials may be achieved by a high aggregate content as well as by using hard and coarse aggregates. Hence, for the SHCC tested here a low abrasion resistance is not surprising since the material is characterized by a low aggregate content and small particle sizes.

However, an SHCC has been used in 2002 in a pilot application for repair layers on outdoor concrete surfaces which are subjected to high wheel loads (ECC, 2009). A particular repair patch was monitored for five years, without any significant abrasion observed. From this result it may be argued that in areas where vehicles travel freely, and no frequent braking occurs, SHCC performs well in terms of abrasion.

## 2.9 Self-healing of Micro-cracks

The fine cracks in SHCC afford these materials the potential of self-healing. It has been shown that a small crack width is imperative for self-healing of concrete (Edwardsen, 1999). Although no systematic study of this phenomenon in SHCC has been reported yet, preliminary observations indicate that SHCC specimens have a self-healing tendency. SHCC specimens of type reference number 8 (Table 2.1) used in water permeability tests (Lepech and Li, 2005) exhibit self-healing, as shown in Figure 2.21. Preliminary studies by Yang et al. (2005) and Li and Yang (2007) indicated the ability of SHCC material to regain both mechanical (strength, stiffness and ductility) and transport properties. In Chapter 3, where durability under chemical action is reported, recent research results on self-healing are discussed (in Section 3.2.3) with particular reference to a marine environment.

A systematic research program is warranted to confirm this phenomenon.

## References

- Arakawa, T. and Ohno, K. (1957). *Transactions of the Architectural Institute of Japan*, 57, pp. 581–584 [in Japanese].
- Bažant, Z.P. and Najjar, L.J. (1971). Drying of concrete as a non-linear diffusion problem, *Cement and Concrete Research*, 1, pp. 461–473.
- Boshoff, W.P. (2007). Time-dependent behaviour of ECC, PhD Dissertation, Stellenbosch University, South Africa.
- Boshoff, W.P. and van Zijl, G.P.A.G. (2006). Time-dependent response of ECC: Characterisation and modeling of creep and creep fracture, in *Proceedings of the Workshop on HPRCC in Structural Applications*, Honolulu, Hawaii, USA, May 23–26, 2005, pp. 125–134.
- Carino, N.J. and Clifton, J.R. (1995). *Prediction of Cracking in Reinforced Concrete Structures*. Report NISTIR 5634, April 1995, Building and Fire Research Laboratory National Institute of Standards and Technology Gaithersburg, MD 20899.
- CEB-FIP (1978). *Model Code for Concrete Structures, CEB-FIP Recommendations*, 3rd edition, Comité Euro-International du Béton Paris, 348 pp.
- DIN EN 13813 (2003). Estrichmörtel, Estrichmassen und Estriche – Eigenschaften und Anforderungen, January. E DIN 52108 (2006). Prüfung anorganischer nichtmetallischer Werkstoffe – Verschleißprüfung mit der Schleifscheibe nach Böhme – Schleifscheiben-Verfahren, Blueprint, January.
- ECC (2009). [http://www.engineeredcomposites.com/Applications/bridge\\_deck.html](http://www.engineeredcomposites.com/Applications/bridge_deck.html), accessed January 2009.
- Edwardsen, C. (1999). Water permeability and autogenous healing of cracks in concrete, *ACI Materials Journal*, 4, pp. 448–454.
- Iosipescu, N. (1967). New accurate method for single shear testing of metals, *J. Materials*, 2(3), pp. 537–566.
- Jun, P. and Mechtcherine, V. (2007). Behaviour of SHCC under repeated tensile loading, in *RILEM PRO 53: HPRCC5*, Mainz, Germany, pp. 97–104.
- Kanda, T. and Li, V.C. (1998). Multiple cracking sequence and saturation in fiber reinforced cementitious composites, *Concrete Research and Technology, JCI*, 9(2), pp. 19–33.
- Kanda, T. and Li, V.C. (1999). A new micromechanics design theory for pseudo strain-hardening cementitious composite. *ASCE J. Eng. Mech.*, 124(4), pp. 373–381.

- Kistutaka, Y. and Tamura, M. (2006). Durability on the fracture parameters of crack repaired high performance fiber reinforced cementitious composites, in *Proceedings of the Workshop on HPFRCC in Structural Applications*, Honolulu, Hawaii, USA, May 23–26, 2005.
- Kunieda, M. and Rokugo, K. (2006). Measurement of crack opening behaviour within ECC under bending moment, in *Proceedings of the Workshop on HPFRCC in Structural Applications*, Honolulu, Hawaii, USA, May 23–26.
- Kunieda, M., Denarié, E., Brühwiler, E., and Nakamura, H. (2007). Challenges for SHCC – Deformability versus matrix density, in *Proc. RILEM PRO 53: HPFRCC5*, Mainz, Germany, pp. 31–38.
- Lawler, J.S., Zampini, D., and Shah, S.P. (2002). Permeability of cracked hybrid fiber reinforced mortar under load, *ACI Materials Journal*, 99(4), pp. 379–385.
- Lepech, M. and Li, V.C. (2005). Water permeability of cracked cementitious composites, in *Proceedings of ICF11*, Turin, Italy, March 2005, pp. 113–130.
- Li, V.C. (1993). From micromechanics to structural engineering – The design of cementitious composites for civil engineering applications, *JSCE Journal of Structural Mechanics and Earthquake Engineering*, 10(2), pp. 37–48.
- Li, V.C. (1998). Engineered cementitious composite (ECC)-tailored composites through micromechanical modelling, in *Fiber Reinforced Concrete: Present and the Future*, N. Banthia, A. Bentur, and A. Mufti (Eds.), Canadian Society for Civil Engineering, Montreal, pp. 64–97.
- Li, V.C. (2002). Reflections on the research and development of Engineered Cementitious Composites (ECC), in *Proceedings of the JCI International Workshop on Ductile Fiber Reinforced Cementitious Composites (DFRCC) – Application and Evaluation (DRFCC-2002)*, Takayama, Japan, October 2002, pp. 1–21.
- Li, V.C. and Lepech, M. (2005). Engineered cementitious composites: Design, performance and applications, in *Ultra-ductile Concrete with Short Fibres – Development, Testing, Applications*, V. Mechtcherine (Ed.), ibidem Verlag, Stuttgart, Germany, pp. 99–120.
- Li, V.C. and Lepech, M. (2006). Durability and long term performance of Engineered Cementitious Composites, in *Proceedings of International Workshop on HPFRCC in Structural Applications*, Honolulu, Hawaii, USA, May 23–26, 2005.
- Li, V.C. and Stang, H. (2004). Elevating FRC material ductility to infrastructure durability, in *Proceedings 6th RILEM Symposium on Fiber-Reinforced Concretes (FRC)*, BEFIB 2004, Varenna, Italy, 20–22 September 2004, pp. 171–186. Varenna, Italy,
- Li, V.C. and Yang, E. (2003). Damage mechanics of Engineered Cementitious Composites, in *Proceedings of NSF-FHWA Workshop on Imaging and Simulation of Concrete Microstructure (Nano to Mesoscale)*, Evanston, IL, pp. 33–37.
- Li, V.C. and Yang, E.H. (2007). Self-healing in concrete materials, in *Self Healing Materials: An Alternative Approach to 20 Centuries of Materials Science*, S. van der Zwaag (Ed.), Springer, pp. 161–193.
- Li, V.C., Mishra, D.K., Naaman, A.E., Wigh, J.K., LaFave, J.M., Wu, H.C., and Inada, Y. (1994). On the shear behavior of engineered cementitious composites, *Journal of Advanced Cement Based Materials*, 1(3), pp. 142–149.
- Li, V.C. Mishra, D.K., and Wu, H.C. (1995). Matrix design for pseudo strain-hardening FRCC, *Materials and Structures*, 28, pp. 586–595.
- Li, V.C., Lim, Y.M., and Chan, Y-W. (1998). Feasibility study of a passive smart self-healing cementitious composite, *Composites, Part B*, 29B, pp. 819–827.
- Li, V.C., Wang, S., and Wu, C. (2001). Tensile strain-hardening behaviour of Polyvinyl Alcohol Engineered Cementitious Composites (PVA-ECC). *ACI Materials Journal*, November/December, pp. 483–492.
- Li, V.C., Wu, C. Wang, S., Ogawa, A., and Saito, T. (2002). Interface tailoring for strain-hardening polyvinyl Alcohol Engineered Cementitious Composite (PVA-ECC), *ACI Materials Journal*, September/October, pp. 463–472.
- Li, V.C., Horikoshi, T., Ogawa, A., Torigoe, S., and Saito, T. (2004). Micromechanics-based durability study of Polyvinyl Alcohol-Engineered Cementitious Composite. *ACI Materials Journal*, May/June, pp. 242–248.

- Maalej, M., Ahmed, S.F.U., and Paramasivam, P. (2002). Corrosion durability and structural response of functionally-graded concrete beams. *J. Adv. Concr. Technol.*, 1(3), pp. 307–316.
- Matsumoto, T., Chun, P., and Suthiwarapirak, P. (2004). Effect of fibre fatigue rupture on bridging stress degradation in fibre reinforced cementitious composites, in *Proceedings of Fracture Mechanics of Concrete Structures*, V.C. Li et al. (Eds.), pp. 653–660.
- Michigan Department of Transportation (MDOT) (2001). Michigan Test Method 111 – Determining an Aggregate Wear Index (AWI) by Wear Track Polishing Tests, Lansing Michigan.
- Miyazato, S. and Hiraishi, Y. (2005). Transport properties and steel corrosion in ductile fiber reinforced cement composites, in *Proceedings of ICF11*, Turin, Italy, March 2005.
- Neithalath, N. (2006). Analysis of moisture transport in mortars and concrete using sorption-diffusion approach, *ACI Materials Journal*, 103(3), pp. 209–217.
- NT BUILD 492 (1999). Concrete, Mortar and Cement-Based Repair Materials: Chloride Migration Coefficient from Non-Steady-State Migration Experiments, Nordtest, Finland.
- Oh, B.H. and Shin, K.J. (2006). Cracking, ductility and durability characteristics of HPFRCC with various mixture proportions and fibers, in *Proceedings of the Workshop on High Performance Fibre Reinforced Cement-based Composites*, Honolulu, Hawaii, May 22–27, 2005.
- Peled, A. and Shah, S.P. (2003). Processing effect in cementitious composites: Extrusion and casting, *Journal of Materials in Civil Engineering*.
- Rapoport, J., Aldea C., Shah, S.P., Ankenman, B., and Karr, A.F. (2001). *Permeability of Cracked Steel Fiber-Reinforced Concrete*. Technical Report Number 115, National Institute of Statistical Sciences, January.
- Sahmaran, M., Li, M., and Li, V.C. (2007). Transport properties of engineered cementitious composites under chloride exposure, *ACI Materials Journal*, 104(6), pp. 604–611.
- Song, G. and van Zijl, G.P.A.G. (2004). Tailoring ECC for commercial application. in *Proceedings 6th Rilem Symposium on Fibre reinforced Concrete (FRC)*, Varenna, Italy, pp. 1391–1400.
- Suthiwarapirak, P., Matsumoto, T., and Kanda, T. (2002). Flexural fatigue failure characteristics of an engineered cementitious composite and polymer cement mortars, *J. Mater., Conc. Struct. Pavements, JSCE*, 57(718), pp. 121–134.
- Tsukamoto, M. (1990). Tightness of fiber concrete, *Darmstadt Concrete*, 5, pp. 215–225.
- Van Zijl, G.P.A.G. (2005). The role of aggregate in HPFRCC. *Concrete/Beton*, 110, pp. 7–13.
- Van Zijl, G.P.A.G. (2007). Improved mechanical performance: Shear behaviour of strain hardening cement-based composites (SHCC). *Cement and Concrete Research*, 37(8), pp. 1241–1247.
- Wagner, C. (2007). Nachverfestigendes zementgebundenes Material für die Sanierung gerissener Betonoberflächen (Strain hardening cement-based material for the repair of cracked concrete surfaces). Master Thesis, Leipzig University of Applied Sciences, Germany.
- Wang, S. and Li, V.C. (2004). Tailoring of pre-existing flaws in ECC matrix for saturated strain hardening, in *Proceedings Fracture Mechanics of Concrete Structures*, V.C. Li et al. (Eds.), pp. 1005–1012.
- Wang, S. and Li, V.C. (2006). Polyvinyl Alcohol Fiber reinforced engineered cementitious composites: Material design and performances, in *Proceedings of International workshop on HPFRCC in Structural Applications*, Honolulu, Hawaii, USA, May 23–26, 2005.
- Wang, K., Jansen, D.C., Shah, S., and Karr, A.F. (1997). Permeability study of cracked concrete, *Cement and Concrete Research*, 27(3) pp. 381–393.
- Weimann, M.B. and Li, V.C. (2003). Hygral behavior of Engineered Cementitious Composites (ECC), *International Journal for Restoration of Buildings and Monuments*, 9(5), pp. 513–534.
- Wittmann, F.H. and Van Zijl, G.P.A.G. (2006). Task Group B – Durability of SHCC conclusions, in *Proceedings Rilem International Workshop on High Performance Fiber Reinforced Cement-Based Composites (HPFRCC) in Structural Applications*, Honolulu, Hawaii, May 22–27, pp. 109–114.
- Yang, Y., Lepech, M., and Li, V.C. (2005). Self-healing of engineered cementitious composites under cyclic wetting and drying, in *Proceedings of International Workshop on Durability of Reinforced Concrete under Combined Mechanical and Climatic Loads (CMCL)*, Qingdao, China, pp. 231–242.

Zang and Li, V.C. (2002). Monotonic and fatigue performance in bending of fiber-reinforced engineered cementitious composite in overlay system, *Cement and Concrete Research*, 32, pp. 415–423.

Durability of Strain-Hardening Fibre-Reinforced  
Cement-Based Composites (SHCC)

van Zijl, G.P.A.G.; Wittman, F.H. (Eds.)

2011, XII, 140 p., Hardcover

ISBN: 978-94-007-0337-7